ROBUST MATERIAL IDENTIFICATION IN HYPERSPECTRAL DATA VIA MULTIRESOLUTION WAVELET TECHNIQUES

John D. Gorman, Nikola S. Subotic, and Brian J. Thelen

Environmental Research Institute of Michigan, Box 134001, Ann Arbor, MI, 48113-4001
Voice: (313) 994-1200, FAX: (313) 994-5704, Email: gorman@erim.org

ABSTRACT

We review the characteristics of hyperspectral imaging sensors and describe several important data exploitation applications in remote sensing. We then focus on a particular signal processing application, material identification, and propose a novel algorithm based on multiresolution wavelet techniques. Finally, we demonstrate the multiresolution material identification algorithm on data collected with a 211-band hyperspectral sensor.

1. BACKGROUND

Hyperspectral imaging sensors collect multiband imagery spanning the visible and infrared portions of the electromagnetic spectrum. Hyperspectral sensors are typically designed to collect simultaneous image bands over contiguous spectral bands, each band having a narrow relative fractional bandwidth that is commonly less than 1%. The result is that a hyperspectral imaging sensor can record a fine spectral resolution electromagnetic profile of each pixel in the field of view. These profiles can then be used to infer properties of materials within each pixel in a scene. More specifically, characteristic wavelength-dependent changes in the emissivity and reflectivity of a given material can be related to the chemical composition and types of atomic and molecular bonds present in that material [3]. Applications of hyperspectral imaging sensors include earth science applications such as environmental monitoring, geodesy, bathymetry, hydrography, soil analysis, and land use surveys, as well as defense applications such as surveillance and treaty verification.

Multispectral features in the reflectivity and emissivity of a material are largely due to changes in the material's complex index of refraction as a function of wavelength. The most prominent features occur at resonant frequencies where the material undergoes electronic and/or vibratory energy transitions at the atomic and/or molecular levels. At infrared wavelengths for instance, these spectral features are largely due to the different types of molecular bonds present in the material. Thus, differences between the spectral profiles of man-made objects and various natural backgrounds can largely be attributed to differences in their chemical composition [2, 3, 5].

Figure 1 shows the hemispheric reflectance spectra of two materials, green paint and grass. One can see significant differences between the spectra in several regimes, a difference in the waveform rise around 0.7 μm, as well as the effect of water vapor absorption in the grass at 1.4 and 1.9 μm. Multispectral and hyperspectral sensors allow exploitation of these material differences through the simultaneous collection of several spectral bands.

2. MODEL

The material identification problem is that of classifying each pixel in a scene according to its material content. Two difficulties that limit the performance of classical classification algorithms are the appearance of multiple material types within a pixel, the so-called "mixed pixel" problem, and the large dimensionality of the hyperspectral signatures. The mixed pixel problem leads to a composite hypothesis testing problem, while the signature dimensionality problem can lead to algorithm robustness problems. As an example, the AVIRIS sensor simultaneously collects 224 spectral bands, each with a 10nm bandwidth distributed over the 0.4 to 2.4μm range [3, 4].

In the hyperspectral remote sensing literature, the material identification problem is commonly referred to as "spectral tagging." Two components of spectral tagging are "endmember selection," determining the constituent components of a mixed pixel, and "abundance

This research supported in part by ERIM internal research and development funds.

0-7803-2431-5/95 $4.00

selection," estimating the relative fraction of each constituent within a pixel [1, 2, 5].

Let $D_{ij;k}$ denote the measurement at pixel (i,j) of the kth spectral band. We assume that the measurement $D_{ij;k}$ can be related to the reflectivity $R_{ij;k}$ of the scene according to the following model:

$$D_{ij;k} = g_{ij;k} R_{ij;k} + o_{ij;k}. \quad (1)$$

Factors $g_{ij;k}$ and $o_{ij;k}$ contain factors which must be corrected for through sensor calibration and data normalization to remove environmental effects. In particular, $g_{ij;k}$ contains scale factors due to non-uniform sensor gain, atmospheric attenuation (i.e., absorption due to moisture vapor) and non-uniform illumination effects (i.e., sun angle effects). The bias or offset term $o_{ij;k}$ accounts for effects such as sensor bias and non-uniform background radiance. We assume that calibration and data normalization has been performed and work directly with the reflectance values $R_{ij;k}$. Reference [4] contains a description of calibration procedures for the AVIRIS sensor; reference [6] contains information on data normalization techniques.

Let $\underline{R}_{ij} = [R_{ij;1}, \ldots, R_{ij;L}]$ denote the vector of spectral reflectance measurements at a given pixel (i,j). It is common to assume that each measured reflectance is a convex mixture of several distinct spectral signatures. In particular, we assume that each $\underline{R}_{ij}$ can be decomposed as the mixture of K *reference spectra*:

$$\underline{R}_{ij} = \sum_{k=1}^{K} \alpha_{ij;k} \underline{S}_k = \underline{\alpha}_{ij}^T \mathbf{S}. \quad (2)$$

Here,

$$\sum_k \alpha_{ij;k} = 1,$$

for each ij, $\underline{\alpha}_{ij} = [\alpha_{ij;1}, \ldots, \alpha_{ij;K}]^T$, and $\mathbf{S} = [\underline{S}_1, \ldots, \underline{S}_K]$.

Two problems that arise in hyperspectral data analysis are the selection of reference spectra, $\underline{S}_1, \ldots \underline{S}_K$, typically referred to as *endmember selection*; and estimation of $\underline{\alpha}_{ij}$, or *abundance estimation* [2, 5]. Sometimes the reference spectra are taken from databases of spectral measurements of specific materials such as minerals, soil, paint and vegetation [2]. Other times the reference spectra, or endmembers, are extracted directly from the imagery using principal component-type analysis [1, 5].

In these latter analyses, the reference spectra are typically treated as *non-random* vectors, and a least-squares approach is used to estimate $\underline{\alpha}_{ij}$ as the *projection* of the measured reflectance data $\underline{R}_{ij}$ onto the matrix $\mathbf{S}$ of reference spectra. On the other hand, it might be more appropriate to model the reflectance $\underline{R}_{ij}$ as a convex combination of *random* spectra, to more accurately model measurement variations due to scene variability.

We shall assume that the spectra $\underline{S}_k, k = 1, \ldots, K$ are Gaussian random vectors each with a known mean vector, $\underline{\mu}_k$ and known covariance matrix Σ_k [in which case we write $\underline{S}_k \sim \mathcal{N}(\underline{\mu}_k, \Sigma_k)$]. The measurements $\underline{R}_{ij}$ in (2) then become convex combinations of Gaussian random vectors. The material identification problem then becomes that of estimating the mixture proportions $\underline{\alpha}_{ij}$ for each pixel (i,j) given a set of reference models $\{(\underline{\mu}_k, \Sigma_k), k = 1, \ldots, K\}$.

In the remainder of the paper, we discuss the problem of *optimal band selection*, or dimension reduction. Specifically, we address the problem of representing the model (2) by a smaller-dimensional spectral signature, either by combining adjacent spectral bands, or by deleting bands not required for the particular discrimination task. There are several applications of band selection including dimensionality reduction for data regularization (i.e., to deal with the effects of small data sample size), adaptive band selection for tunable sensors, and data compression. Moreover, the band selection approach we propose may provide an useful alternative to previously proposed principal-component type representations [1, 5].

3. OPTIMAL BAND SELECTION

We consider the problem of optimal band selection in hyperspectral data, or dimension reduction. Specifically, suppose that one knows *a priori* which materials are to be discriminated between in a given AVIRIS image. Which of the 224 spectral bands, or what linear combinations of those 224 bands are required for the discrimination task? What are the minimal number of bands required to achieve a specified discrimination performance? We propose a band selection scheme that uses a min-max selection criterion to reduce the full hyperspectral data set to a small number of linear band combinations that is sufficient to achieve a prespecified discrimination performance. Specifically, we decompose the reference spectra using use a wavelet transform and select the fewest wavelet coefficients required to perform a given discrimination task. These wavelet coefficients then yield a reduced-dimension basis set that can be used to represent the measured reflectance spectra $\underline{R}_{ij}$ in the material identification problem.

Let $W_k(a_m, \lambda_n), m, n = 1, 2, \ldots,$ denote coefficients the *discrete wavelet transform* of spectral reflectance

vector $\underline{S}_k$ along the *spectral* dimension:

$$W_k(a_m, \lambda_n) = \sum_{l=1}^{L} S_k(l) \frac{1}{a_m^{-1/2}} \psi\left(\frac{\eta_l - \lambda_n}{a_m}\right), \quad (3)$$

where $\underline{S}_k = [S_k(1), \ldots, S_k(L)]^T$ and ψ is analyzing wavelet wavelet kernel. The wavelet transform decomposes the hyperspectral signature into a set of *composite bands* which are linear, weighted combinations of the original spectral bands. These linear combinations can be of a very fine scale (single band) to very coarse scales (combinations of many bands). Here, λ_n represents the center frequency of a the band associated with $W_k(a_m, \lambda_n)$ and a_m represents its bandwidth.

The assumption that each of the reference spectra $\underline{S}_k$ is a Gaussian random vector implies that each of the wavelet coefficients is a Gaussian random variable. Let $\underline{W}_k$ be the vector of wavelet coefficients corresponding to spectrum S_k and let $\underline{W}'_k$ denote a subset of these coefficients. We use the shorthand notation $p_k(\underline{W}'_k)$ to denote the probability density function of $\underline{W}'_k$. By assumption, $\underline{W}'_k$ is Gaussian. We use maximum-likelihood techniques to estimate the mean vector and covariance of $p_k(\underline{W}'_k)$.

The distance between two distribution functions, say p_i and p_j is determined via the Kullback-Liebler (cross-entropy) measure as

$$D(p_i, p_j) = \int p_i(\bar{w}) \log \frac{p_i(\bar{w})}{p_j(\bar{w})} d\bar{w} \quad (4)$$

In our case, we select wavelet coefficients (i.e. composite bands) to maximize the *worst case* distance between any pair of materials in the library. Using this distance, we guarantee that the maximum probability of error for the library is minimized.

The band selection is a sequential process. After the wavelet decomposition, an initial pairwise search ($\bar{W}$ is 2D) is made to find the best two bands (wavelet coefficients) which maximizes the minimum cross entropy between the materials. Then given those selected bands, the search continues to find the third best ($\bar{W}$ is 3D), etc. A perturbation method is then used to determine that the previously selected bands are still "the best." This operation continues until either: a) a specific discrimination goal is attained (large enough cross entropy); or b) the maximum number of bands allowed have been selected. This analysis would be done off-line on a reference library of materials. A specific subset of wavelet coefficients would be created for each material library constructed. The coefficient subset would then define a transformation, T, on the input hyperspectral data $\bar{y}' = T\bar{y}$ which reduces its dimensionality. The unknown input data would then be transformed by T producing the new observation vector $\bar{y}'$ which could then be in the endmember selection and abundance estimation problems discussed above.

4. EXAMPLE

We implemented the min-max band selection scheme described above to select band combinations that were optimal for discriminating between paint and vegetation. Data used for this example were taken from the ERIM reflectance data base. This data base spans .4-2.5μm with a resolution of .01μm. 211 bands are present. Two reflectance profiles is shown in Figure 1, olive-drab paint and dry grass. Distinct differences between the two signatures are manifested in two absorption dips at 1.4 and 1.9 μm in the grass signature due to water absorption, and a difference in signature rise at wavelengths around 0.7 μm. The bottom of figure 1 shows the best four bands selected by the algorithm. These four bands correspond directly to bands that would have been selected using heuristic arguments based on reflectance phenomenology. Figure 2 shows a scatter plot of olive drab paint and vegetation signatures over the two best bands selected by the wavelet algorithm. Note the distinct separation between the two populations which will lead to accurate classification performance.

5. SUMMARY

Hyperspectral imaging sensors record fine-resolution electromagnetic profiles of each pixel in the field of view. These profiles can be used to infer properties of materials within each pixel in a scene. We presented a min-max approach for reducing the multichannel hyperspectral imagery to a smaller-dimension collection of linear band combinations that are optimal for material discrimination. Applications of the band selection algorithm include, optimal data reduction, data compression, and band selection for tunable sensors.

6. REFERENCES

[1] J. W. Boardman, "Inversion of Imaging Spectrometry Data Using Singular Value Decomposition," *Proc. IEEE Int'l Geosci. and Remote Sens. Symp*, pp. 2069-2072, 1989.

[2] A. R. Gillespie, M. O. Smith, J. B. Adams, S. C. Willis, A. F. Fischer, and D. E. Sabol, "Interpretation of Residual Images: Spectral Mixture Analysis of AVIRIS Images, Owens Valley, California," *Proc. 2nd AVIRIS Workshop*, JPL Publication 90-54, June 1990.

[3] A. F. H. Goetz, G. Vane, J. E. Solomon and B. N. Rock, "Imaging Spectrometry for Earth Remote Sensing," *Science*, v. 228, no 4704, pp. 1147-1153, June 1985.

[4] R. O. Green, J. E. Conel, C. Bruegge, V. Carrare, J. Margolis, and G. Hoover, "Laboratory Spectral and Radiometric Calibration of AVIRIS," *Proc. Airborne Sci. Workshop: AVIRIS,* JPL, Pasadena CA, June 4-5, 1990.

[5] A. R. Huete, "Separation of Soil-Plant Spectral Measures by Factor Analysis," *Remote Sensing of the Environment*, v. 19, pp. 237-251, 1986.

[6] T. J. Rogne, *Algorithm Development for Multispectral Data Normalization: Phase I,* ERIM Final Technical Report 232300-17-T, Air Force Wright Laboratory, September 1991.

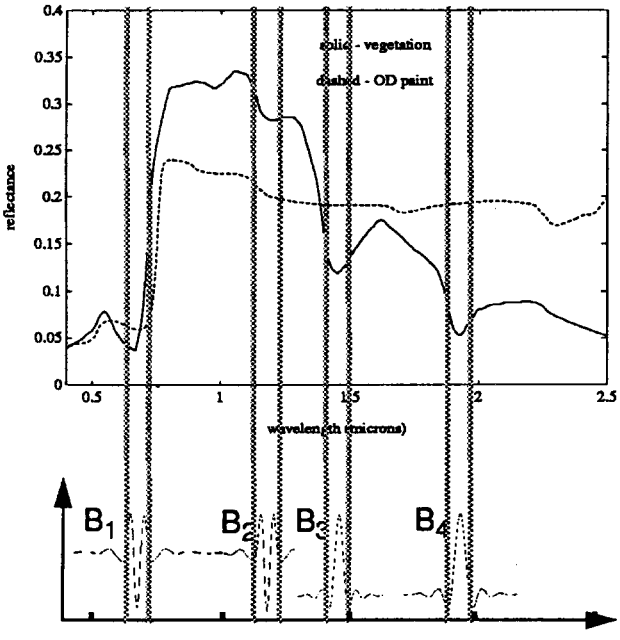

Figure 1: Top: Reflectance spectra of vegetation and olive drab paint; Bottom: Selection of best four composite bands for material characterization via min-max wavelet method.

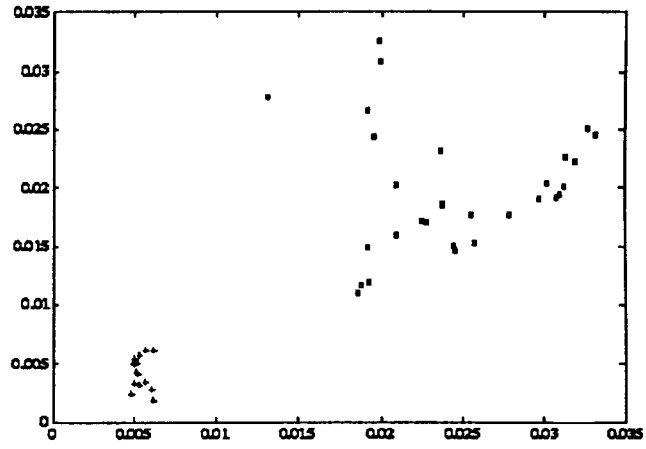

Figure 2: Scatter plot of composite band 1 versus composite band 2 for olive drab paint (+) and vegetation (squares) for two best bands selected by the min-max wavelet decomposition method.